Available online at www.sciencedirect.com
ScienceDirect
Biochemical and Biophysical Research Communications 366 (2008) 988–993
BBRC
www.elsevier.com/locate/ybbrc

Allosterically coupled calcium and magnesium binding sites are unmasked by ryanodine receptor chimeras

Andrew A. Voss [a,1], Paul D. Allen [b], Isaac N. Pessah [a,*], Claudio F. Perez [b]

[a] Department of Molecular Biosciences, School of Veterinary Medicine, University of California, Davis, One Shields Avenue, Davis, CA 95616, USA
[b] Department of Anesthesia Perioperative and Pain Medicine, Brigham and Women's Hospital, 75 Francis Street, Boston, MA 02115, USA

Received 26 November 2007
Available online 26 December 2007

Abstract

We studied cation regulation of wild-type ryanodine receptor type 1 ($_{WT}$RyR1), type 3 ($_{WT}$RyR3), and RyR3/RyR1 chimeras (Ch) expressed in 1B5 dyspedic myotubes. Using [^{3}H]ryanodine binding to sarcoplasmic reticulum (SR) membranes, Ca^{2+} titrations with $_{WT}$RyR3 and three chimeras show biphasic activation that is allosterically coupled to an attenuated inhibition relative to $_{WT}$RyR1. Chimeras show biphasic Mg^{2+} inhibition profiles at 3 and 10 μM Ca^{2+}, no observable inhibition at 20 μM Ca^{2+} and monophasic inhibition at 100 μM Ca^{2+}. Ca^{2+} imaging of intact myotubes expressing Ch-4 exhibit caffeine-induced Ca^{2+} transients with inhibition kinetics that are significantly slower than those expressing $_{WT}$RyR1 or $_{WT}$RyR3. Four new aspects of RyR regulation are evident: (1) high affinity (H) activation and low affinity (L) inhibition sites are allosterically coupled, (2) Ca^{2+} facilitates removal of the inherent Mg^{2+} block, (3) $_{WT}$RyR3 exhibits reduced cooperativity between H activation sites when compared to $_{WT}$RyR1, and (4) uncoupling of these sites in Ch-4 results in decreased rates of inactivation of caffeine-induced Ca^{2+} transients.
© 2007 Elsevier Inc. All rights reserved.

Keywords: Ryanodine receptors; Calcium-induced calcium release; Channel regulation; Regulation of calcium signaling; Skeletal muscle

Three isoforms of wild-type ryanodine receptors ($_{WT}$RyR1, 2 and 3) are expressed in specialized regions of endoplasmic/sarcoplasmic reticulum (ER/SR) in most mammalian cells where they function as Ca^{2+} release channels that produce local and global Ca^{2+} signals [1,2]. Fluctuating physiological cation concentrations, especially Ca^{2+} and Mg^{2+}, tightly regulate the activity of all three $_{WT}$RyR isoforms [3–9]. Cytoplasmic Ca^{2+} ranging from nM to μM enhances the open probability of $_{WT}$RyRs, whereas >100 μM Ca^{2+} or Mg^{2+} depresses channel activity [5,10] and [11]. The "bell shaped" regulation of $_{WT}$RyR by Ca^{2+} is thought to be responsible for physiological and pathophysiological Ca^{2+}-induced Ca^{2+} release (CICR) phenomena observed in many cell types, including muscle and neurons [1,2,12,13] and [14].

$_{WT}$RyR isoforms preferentially bind the plant alkaloid ryanodine with nM affinity when in the open state [3,6] and [7]. Ca^{2+} and Mg^{2+} titrations in [^{3}H]ryanodine binding and Ca^{2+} release experiments have revealed Hill coefficients >1, indicating coordinated regulation of CICR channels by multiple cation binding sites [15]. Mg^{2+} inhibition studied with channels reconstituted in lipid bilayer membranes [16] and Ca^{2+} release from SR membrane vesicles [4] and [11] suggest dual mechanisms of Mg^{2+} inhibition through competition with Ca^{2+} for high affinity (H) activation sites and binding at low affinity (L) cation inhibition sites. At physiological concentrations, free Mg^{2+} (1–2 mM) is likely to occupy both H and L sites, providing a basal level of $_{WT}$RyR inhibition that must be overcome for EC-coupling to occur [17,18]. Studies have suggested that the physical coupling between $_{WT}$RyR and the dihydropyridine receptor (DHPR) may remove the Mg^{2+} block

* Corresponding author. Fax: +1 530 752 4698.
E-mail address: inpessah@ucdavis.edu (I.N. Pessah).
[1] Present address: Department of Physiology, David Geffen School of Medicine, University of California, Los Angeles, CA, USA.

0006-291X/$ - see front matter © 2007 Elsevier Inc. All rights reserved.
doi:10.1016/j.bbrc.2007.12.058

during EC-coupling [18]; whereas, other authors have suggested oxidation of $_{WT}$RyR sulfhydryl groups may override Mg^{2+} inhibition [19]. Functional overlap of Ca^{2+} and Mg^{2+} interactions at H and L regulation sites have confounded cation regulation studies of $_{WT}$RyR1 and resulted in conclusions partially derived from extrapolation. A system that permits more direct analysis of cytoplasmic Ca^{2+} and Mg^{2+} regulation would greatly facilitate mechanistic interpretations of RyR cation regulation in health and disease.

RyR3/RyR1 chimeras were designed to identify regions of $_{WT}$RyR1 directly associated with the DHPR during EC-coupling [20,21]. In this report, [^{3}H]ryanodine binding experiments on $_{WT}$RyR1, $_{WT}$RyR3, and a subset of these chimeras (Ch-4, $_{WT}$RyR$_1$ 1681–3770; Ch-17, 1681–2217; Ch-21, 1924–2446) reveal a biphasic cytoplasmic Ca^{2+} activation profile, suggesting variable cooperativity between H activation sites, revealing coupled but separated interactions at H activation and L inhibition sites. This study provides direct insight into Ca^{2+} and Mg^{2+} regulation, suggests new aspects of $_{WT}$RyR function, and establishes the chimeras as models for future studies of $_{WT}$RyRs and cation regulation.

Materials and methods

Chimeric RyR1/RyR3 constructs. Specific primers were designed for PCR amplification of the selected fragments using $_{WT}$RyR1 as a template. Amplified fragments from $_{WT}$RyR1 encoding aa 1681–2217 (Ch-17), 1924–2446 (Ch-21) and 1681–3770 (Ch-4) were inserted, in frame, into the endogenous restriction site(s) of HSV-RyR3 plasmid as described previously [20]. All chimeric constructs were cloned into the HSV-1 amplicon vector and packaged using a helper virus-free packaging system [22].

Cell culture, infection, and membrane preparation. 1B5 myoblasts were cultured and differentiated into myotubes as described previously [20] and [23]. Plates with differentiated myotubes were infected with virion containing wild-type and RyR1/RyR3 chimeric cDNA for 2 h and membrane extracts were prepared 36 h after infection. Myotubes were homogenized and membrane fractions obtained by differential centrifugation as described previously [24].

[^{3}H]Ryanodine binding assay. High affinity binding of [^{3}H]ryanodine ([^{3}H]Ry; 56 Ci/mmol; New England Nuclear, Boston, MA) to membranes (10–50 μg/ml protein) was performed in the presence of 250 mM KCl, 20 mM Hepes, pH 7.4, and 5 nM [^{3}H]Ry [6]. Free Ca^{2+} and Mg^{2+} concentrations buffered with EGTA were determined using the Bound And Determined software [25]. The binding reaction was equilibrated at 37 °C for 3 h. Non-specific binding was assessed in the presence of 5 μM unlabeled ryanodine. Bound ligand was separated from free by filtration through Whatman GF/B glass fiber filters using a Brandel cell harvester (Gaithersburg, MD), washed with ice-cold buffer, placed into 5 ml scintillation cocktail (ScintiVerse; Fisher Scientific), and radioactivity counted.

Equations for binding analysis. Curve fitting was generated by Microcal™ Origin® Version 6.0 using the equations:

Activation:

$$\text{(a) } y = \frac{(B_{max})(x^n)}{k^n + x^n} \qquad \text{(b) } y = \frac{(B_{max_1})(x^{n_1})}{k_1^{n_1} + x^{n_1}} + \frac{(B_{max_2})(x^{n_2})}{k_2^{n_2} + x^{n_2}}$$

where, B_{max} = maximum bound, $k = EC_{50}$ and n = Hill coefficient

Inhibition:

$$\text{(c) } y = \frac{A_1 - A_2}{1 + (\frac{x}{xo})^p} + A_2 \qquad \text{(d) } y = A_2 + \frac{(A_1 - A_2)f}{1 + 10^{(x - \log xo_1)}} + \frac{(A_1 - A_2)(1-f)}{1 + 10^{(x - \log xo_2)}}$$

where A1 = top asymptote, A2 = bottom asymptote, xo = IC50, f = fraction, and p = power.

Ca^{2+} imaging. Calcium imaging was performed during the stable phase of transduced protein expression in the myotubes 36–48 h post-infection as previously described [20]. Ca^{2+} release was induced with 20 s perfusion of 20 mM caffeine. Monophasic exponential decay curves were fitted with GraphPad Prism® Version 4.0 according to following function: $y = Span \cdot e^{(-k \cdot X)} + Plateau$ were k = rate constant.

Results and discussion

To examine cation regulation, both $_{WT}$RyRs and RyR3/RyR1 chimeras were expressed in dyspedic 1B5 myotubes, a myogenic cell line devoid of all $_{WT}$RyR isoforms, but containing the accessory proteins necessary for normal $_{WT}$RyR function [26]. Regulation of $_{WT}$RyRs and chimeras in membrane fractions was assessed using [^{3}H]Ry binding to probe cation regulation of channel conformation permitting direct analysis of cytoplasmic Ca^{2+} and Mg^{2+} regulation of RyR conformation [6] without confounding influences of varying luminal Ca^{2+} [27].

Ca^{2+} regulation

Ca^{2+} activation of $_{WT}$RyR1 and $_{WT}$RyR3 determined by [^{3}H]Ry binding (Fig. 1A) indicated monophasic activation of $_{WT}$RyR1 ($EC_{50} = 0.54 \pm 0.05$ μM) and biphasic activation of $_{WT}$RyR3 ($EC_{50(1)}$ and $EC_{50(2)} = 0.36 \pm 0.06$ μM and 20.0 ± 5.78 μM) with a plateau from 4–8 μM (inset). Similar analyses of Ch-21, -17 and -4 revealed accentuated biphasic Ca^{2+} responses, with plateaus of 20–100 μM, 10–100 μM, and 3–100 μM, respectively (Fig. 1B). Ch-21, -17 and -4 exhibited $EC_{50(1)}$ values of 0.90 ± 0.19 μM, 0.39 ± 0.09 μM and 0.18 ± 0.03 μM, and $EC_{50(2)}$ values of 397 ± 190 μM, 510 ± 174 μM, and 761 ± 192 μM, respectively (Table 1).

The biphasic profiles suggest $_{WT}$RyR3 and chimeras possess reduced cooperativity between H activation sites compared to $_{WT}$RyR1. The Ca^{2+} dependence of $_{WT}$RyR3 has been previously published based on immunoprecipitated protein and the resulting data fitted using a single-site model indicating monophasic activation of $_{WT}$RyR3 by Ca^{2+} [28] and [29]. Two significant methodological differences distinguish the present study. First, the use of SR membranes from $_{WT}$RyR3-expressing 1B5 myotubes preserves known interactions with lumenal proteins such as calsequestrin [26] that are known to contribute to cation regulation of $_{WT}$RyR1 and $_{WT}$RyR2 [27] and [30]. Second, the extremely broad titrations in previous studies with immunopurified $_{WT}$RyR3 consisted of 2–4 data points covering several log range of Ca^{2+} concentrations and would have missed the biphasic activation of $_{WT}$RyR3 by Ca^{2+} if present after immunopurification. The present study is the first report of a distinctly biphasic activation for $_{WT}$RyR3 and may result from an altered conformation relative to $_{WT}$RyR1 that is exaggerated in the chimeras. A slight variation in protein conformation would explain the deviation in chimeric Ca^{2+} activation from that of

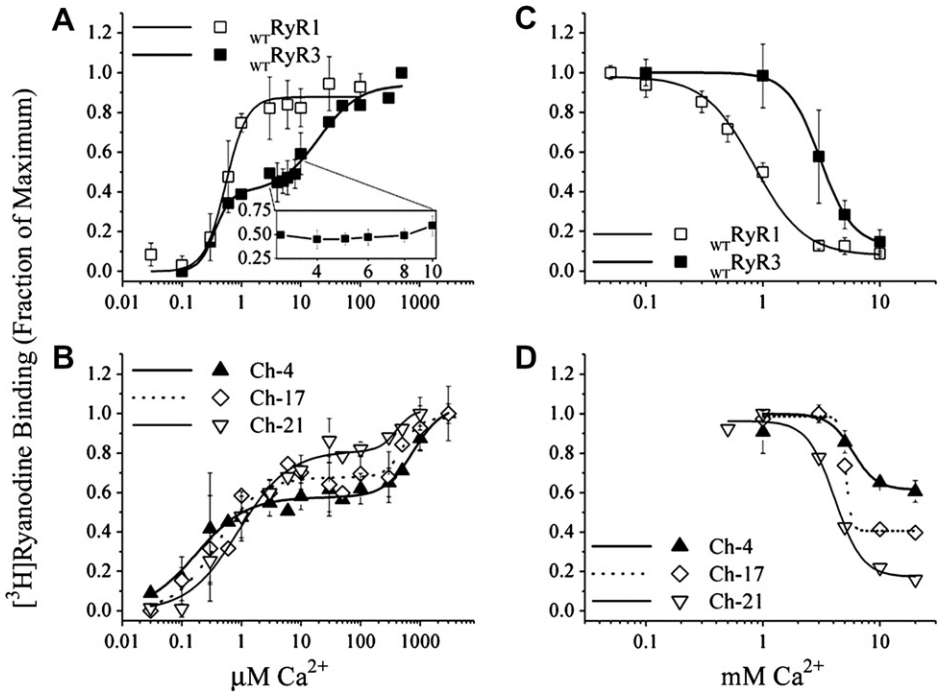

Fig. 1. Ca^{2+} regulation of wild-type and chimeric RyR3/RyR1 expressed in dyspedic 1B5 myotubes, determined by [^{3}H]Ry binding (see Methods). (A) Activation of RyR1 (—□—) and RyR3 (—■—) curve fit with Hill and biphasic Hill equations, respectively. (B) Activation of Ch-4 (—▲—), Ch-17 (---◊---), and Ch-21 (—∇—) curve fit with a biphasic Hill equation. (C) Inhibition of RyR1 (—□—) and RyR3 (—■—) curve fit with a monophasic equation. (D) Inhibition of Ch-4 (—▲—), Ch-17 (---◊---), and Ch-21 (—∇—) with a biphasic equation. Data points are the mean values, error bars are ± standard deviations. Activation profiles for $_{WT}$RyR1, $_{WT}$RyR3 and Ch-4 were the combined result of 2–4 experiments performed in duplicate or triplicate from multiple 1B5 membrane preparations.

Table 1
Curve fit statistics for [^{3}H]Ry binding analyses of Ca^{2+} activation

Construct	$EC_{50(1)}$ (μM)	$EC_{50(2)}$ (μM)	Hill coeff. 1	Hill coeff. 2	r^2
$_{WT}$RyR1	0.54 ± 0.05	N/A	2.42 ± 0.48	N/A	0.982
$_{WT}$RyR3	0.36 ± 0.06	20.0 ± 5.78	3.26 ± 1.75	1.29 ± 0.40	0.985
Ch-4	0.18 ± 0.03	761 ± 192	1.04 ± 0.17	1.78 ± 0.65	0.986
Ch-17	0.39 ± 0.09	510 ± 174	1.20 ± 0.33	3.08 ± 2.90	0.961
Ch-21	0.90 ± 0.19	397 ± 190	1.03 ± 0.19	3.06 ± 4.32	0.985

$_{WT}$RyR1 and 3, an unpredictable response based on primary sequence alone. It is also noteworthy that previously published whole cell Ca^{2+} imaging experiments indicate these chimeras expressed in 1B5 cells are functional, with all three constructs exhibiting calcium-induced Ca^{2+} release (CICR) and Ch-4 and -21 additionally engaging skeletal-type EC-coupling [20]. Interestingly, a recent [^{3}H]Ry-binding study with membranes isolated from rat ventricular muscle showed a similar biphasic Ca^{2+} activation curve for RyR2, which was reverted to a monophasic binding profile in the presence of Mg^{2+} [31]. Collectively these results support a mechanism by which coordinated Ca^{2+} activation sites regulate RyR conformations that bind ryanodine with high affinity.

[^{3}H]Ry binding analysis of Ca^{2+} inhibition through L sites revealed an attenuated response that correlates to H site cooperativity (Fig. 1C and D). Compared to $_{WT}$RyR1, multiple aspects of Ca^{2+} inhibition were shifted in $_{WT}$RyR3 and chimeric constructs. First, the onset of inhibition is attenuated in $_{WT}$RyR3 and Ch-21 to ~1 mM and in Ch-17 and -4 to ~3–4 mM vs. $_{WT}$RyR1 at 100 μM. Additionally, the extent of inhibition observed in the chimeras is shifted, where Ch-21, -17, and -4 were, respectively, 84%, 60%, and 39% of the near complete inhibition observed in $_{WT}$RyR1 and $_{WT}$RyR3. Finally, as summarized in Table 2, the IC_{50} values suggested attenuated inhibition

Table 2
Curve fit statistics for [^{3}H]Ry binding analyses of Ca^{2+} inhibition

Construct	IC_{50} (mM)	r^2
$_{WT}$RyR1	0.84 ± 0.08	0.997
$_{WT}$RyR3	3.08 ± 0.88	0.999
Ch-4	5.86 ± 1.18	0.985
Ch-17	5.09 ± 4.13	0.999
Ch-21	4.11 ± 0.27	0.994

compared to $_{WT}$RyR1 (0.84 ± 0.08 mM) in $_{WT}$RyR3 (3.08 ± 0.88 mM), Ch-21 (4.11 ± 0.27 mM), Ch-17 (5.09 ± 4.13 mM) and Ch-4 (5.86 ± 1.18 mM) (Table 2). The extent of attenuated Ca^{2+} inhibition through L sites appeared related to H site cooperativity, in which channels with the greatest reduction in H site cooperativity exhibit the largest attenuation in L site mediated inhibition. These data strongly suggests H and L sites are allosterically coupled.

The observations presented heretofore illustrate a model of RyR regulation by Ca^{2+} in which the binding of at least one H site by Ca^{2+} induced a plateau in [^{3}H]Ry binding. This plateau was undetected in $_{WT}$RyR1 due to cooperative binding of Ca^{2+} to at least one additional H site, but was observed in $_{WT}$RyR3 and further exacerbated in chimeras where there was a reduction in cooperativity between H sites. Binding of Ca^{2+} to the additional H site(s) induced a conformational transition to a state of maximal ryanodine binding. Further increases of Ca^{2+} occupied L sites and decreased [^{3}H]Ry binding. This data indicates H and L sites are allosterically coupled, as the onset of L site mediated inhibition did not occur until complete H site occupation, and complete inhibition through L sites required near-complete cooperativity between H sites.

Mg^{2+} inhibition

In light of Ca^{2+} regulation through coupled but separated H and L sites, we examined with [^{3}H]Ry the role of Mg^{2+} in Ch-4 cation regulation (Fig. 2; Table 3), with curve statistics summarized in Table 3. In the presence of 3 and 10 μM Ca^{2+}, Mg^{2+} produced biphasic responses with $IC_{50(1)}$ values of 0.40 ± 0.13 mM and 0.64 ± 0.09 mM, respectively. The $IC_{50(2)}$ values for Mg^{2+} at 3 and 10 μM Ca^{2+} were 5.71 ± 0.31 mM and 4.18 ± 0.16 mM, respectively. At 100 μM Ca^{2+}, the first phase of Mg^{2+} inhibition

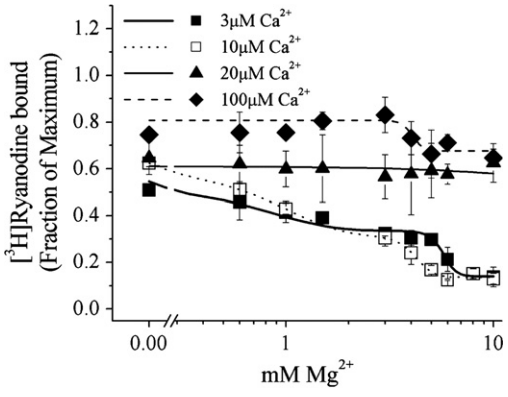

Fig. 2. Mg^{2+} inhibition at variable Ca^{2+} of Ch-4 expressed in dyspedic 1B5 myotubes, determined by ^{3}H-ryanodine binding (see Methods). In the presence of 3 (—■—) and 10 μM (···□···) Ca^{2+} curve fit with a biphasic equation. In the presence of 20 μM Ca^{2+} (—▲—) fit linearly ($m = -0.0032 \pm 0.0029$ and $b = 0.611 \pm 0.015$) and at 100 μM Ca^{2+} (---♦---) curve fit with a monophasic equation. Data points are mean values for at least two experiments, error bars are ± standard deviations.

Table 3
Curve fit statistics for [^{3}H]Ry binding analyses of Ch-4 Mg^{2+} inhibition at variable Ca^{2+}

[Ca^{2+}]	$IC_{50(1)}$ (mM)	$IC_{50(2)}$ (mM)	r^2
3 μM	0.40 ± 0.13	5.71 ± 0.31	0.964
10 μM	0.64 ± 0.09	4.18 ± 0.16	0.998
20 μM	No Inhibition		
100 μM	4.06 ± 0.40	N/A	0.881

was not detected and only an incomplete (~40% of maximum), monophasic inhibition ($IC_{50} = 4.06 \pm 0.40$ mM) was observed. The biphasic Mg^{2+} profiles at 3 and 10 μM Ca^{2+} likely represent competition with Ca^{2+} for H sites in the first phase and binding to L sites in the second. Competition by Mg^{2+} for H sites is supported by a shifting first phase for Mg^{2+} inhibition at 3 and 10 μM Ca^{2+} that is not observed at 100 μM Ca^{2+}. Binding of Mg^{2+} to L sites is described by a monophasic inhibition at 100 μM Ca^{2+} ($IC_{50} = 4$–6 mM), a range that corresponds to the observed Ca^{2+} inhibition through L sites (5.86 ± 1.18 mM) in Fig. 1D. These results provide more direct biochemical evidence in support of the dual mechanism of Mg^{2+} inhibition originally proposed by Meissner and Laver based on experiments with $_{WT}$RyR [4,16] and [32].

An intriguing finding was that Mg^{2+} titrations in the presence of 20 μM Ca^{2+} produced no observable inhibition in [^{3}H]Ry binding experiments. Loss of Mg^{2+} inhibition would be possible through competition at H sites and a conformational state at the Ca^{2+} biphasic plateau, which reduces the affinity of Mg^{2+} at L sites relative to conformations at low (3 and 10 μM) and high (100 μM) Ca^{2+}. Alternatively, Mg^{2+} binding could impart an activating effect on H sites, as suggested for rat RyR2 [31]. This further supports allosteric coupling between H and L sites and suggests Ca^{2+} may contribute along with DHPR [18] and oxidation [19] to relieving the inherent physiological block provided by Mg^{2+}.

Physiological relevance of the observations presented in this work depend on the idea that chimeric characteristics unmasked by the reduced H site cooperativity are inherent to $_{WT}$RyR, but are difficult to observe in wild-type (especially $_{WT}$RyR1) due to overlapping interactions at H and L sites. For $_{WT}$RyR3 however, the present results would predict unique functional effects at Ca^{2+} concentrations corresponding to the activation plateau (4–8 μM) shown in Fig. 1A. Indeed, at 5–10 μM Ca^{2+}, $_{WT}$RyR3 was shown to exhibit increased subconductance behavior relative to $_{WT}$RyR1 [28] and [33]. This correlation is additionally supported by increased subconductance behavior of brain $_{WT}$RyRs at specific Ca^{2+} and ATP concentrations [34].

Ca^{2+} release from SR stores

To extend the [^{3}H]Ry binding results, we examined the effect of altered Ch-4 cation regulation on Ca^{2+} release in transduced 1B5 myotubes. In these cells, transduced Ch-4

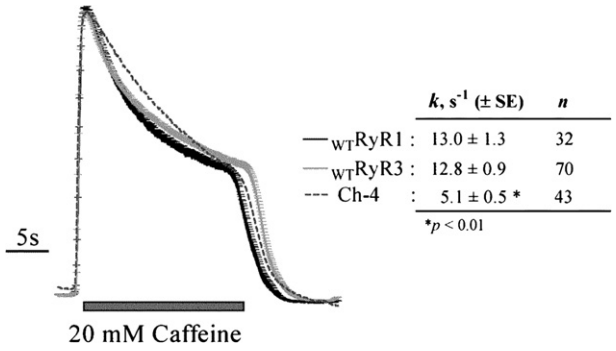

Fig. 3. Caffeine-induced Ca^{2+} release kinetics of 1B5 myotubes expressing Ch-4, $_{WT}$RyR1 or $_{WT}$RyR3. Average Ca^{2+} transients, normalized by the peak amplitude, are presented for each construct (mean ± SE). For clarity trend line for Ch-4 is displayed without SE. Rate constant were calculated using only the decay portion of each Ca^{2+} transient.

was shown to engage skeletal-type EC-coupling and respond to caffeine stimulation [20] and [24]. We therefore compared the kinetics associated with caffeine-induced Ca^{2+} release from myotubes expressing $_{WT}$RyR1, $_{WT}$RyR3, and Ch-4. Since Ch-4 cation inhibition is attenuated at basal levels of intracellular Ca^{2+} or Mg^{2+} due to incomplete occupation of H sites, we predicted a prolonged Ca^{2+} response following a caffeine-induced Ca^{2+} transient for myotubes expressing Ch-4 compared to those expressing $_{WT}$RyR1 or $_{WT}$RyR3. Fig. 3 shows the average Ca^{2+} transients induced by 20 mM caffeine in 1B5 myotubes expressing each construct and loaded with Fluo-4. Upon caffeine application a fast phase of Ca^{2+} release and subsequent slower phase of cytoplasmic Ca^{2+} removal was followed by a fast Ca^{2+} removal phase after caffeine withdrawal. Whereas all constructs showed seemingly identical activation kinetics for caffeine-induced Ca^{2+} release, Ch-4-expressing cells presented a noticeable reduction in the slow Ca^{2+} removal phase and hence prolonged Ca^{2+} response when compared to cells expressing either $_{WT}$RyR1 or $_{WT}$RyR3. Analysis of the slow Ca^{2+} removal phase using a monophasic exponential decay reveals that the rate constant (k) for Ch-4 expressing myotubes is nearly 2.5-fold slower than those measured for $_{WT}$RyR1 or $_{WT}$RyR3 myotubes (Fig. 3). Since saturating concentrations of caffeine were used to induce Ca^{2+} release, the differences in k values observed in this study were most likely associated to the differences in Ca^{2+} and Mg^{2+} regulation of Ch-4 and not to potential differences in sensitivity to the agonist between the three constructs.

Conclusion

The results with RyR1/RyR3 chimeras presented here provide novel insights into the allosteric mechanisms by which Ca^{2+} and Mg^{2+} regulate RyRs, especially interactions between H and L cation binding sites. This allosteric coupling underscores the importance of considering the contribution of Mg^{2+} in addition to Ca^{2+} when assessing RyR function, as physiological levels of Mg^{2+} likely occupy $_{WT}$RyR L sites and may influence Ca^{2+} activation through H sites. Furthermore, these results suggest that observed differences between $_{WT}$RyRs and/or chimeric constructs should be interpreted with awareness of specific channel responsiveness to and the concentrations of Ca^{2+} and Mg^{2+}. This is made apparent by variable responses to the same cation concentrations among wild-type and chimeric RyRs. The contribution of RyR effectors such as FKBP, ATP, DHPR and oxidation in the context of the cation allosteric regulation presented here is yet to be determined. Additionally, the association of subconductance behavior to Ca^{2+} concentrations in the activation plateau needs to be further examined. This work provides new insights into $_{WT}$RyR regulation and function, and establishes RyR chimeras, particularly Ch-4, as a model for future studies of RyR cation regulation and subconductance behavior.

Acknowledgments

This work was supported by 1RO1 AR43140-10A1 (P.D.A. and I.N.P.) and Training Grant T20 ES07059 (AAV) from the National Institutes of Health.

References

[1] M.J. Berridge, Calcium microdomains: organization and function, Cell Calcium 40 (2006) 405–412.
[2] R. Zalk, S.E. Lehnart, A.R. Marks, Modulation of the ryanodine receptor and intracellular calcium, Annu. Rev. Biochem. 76 (2007) 367–385.
[3] I.N. Pessah, A.L. Waterhouse, J.E. Casida, The calcium-ryanodine receptor complex of skeletal and cardiac muscle, Biochem. Biophys. Res. Commun. 128 (1985) 449–456.
[4] G. Meissner, E. Darling, J. Eveleth, Kinetics of rapid Ca^{2+} release by sarcoplasmic reticulum. Effects of Ca^{2+}, Mg^{2+}, and adenine nucleotides, Biochemistry 25 (1986) 236–244.
[5] J.S. Smith, R. Coronado, G. Meissner, Single channel measurements of the calcium release channel from skeletal muscle sarcoplasmic reticulum. Activation by Ca^{2+} and ATP and modulation by Mg^{2+}, J. Gen. Physiol. 88 (1986) 573–588.
[6] I.N. Pessah, R.A. Stambuk, J.E. Casida, Ca^{2+}-activated ryanodine binding: mechanisms of sensitivity and intensity modulation by Mg^{2+}, caffeine, and adenine nucleotides, Mol. Pharmacol. 31 (1987) 232–238.
[7] A. Chu, M. Diaz-Munoz, M.J. Hawkes, K. Brush, S.L. Hamilton, Ryanodine as a probe for the functional state of the skeletal muscle sarcoplasmic reticulum calcium release channel, Mol. Pharmacol. 37 (1990) 735–741.
[8] T. Murayama, Y. Ogawa, Purification and characterization of two ryanodine-binding protein isoforms from sarcoplasmic reticulum of bullfrog skeletal muscle, J. Biochem. (Tokyo) 112 (1992) 514–522.
[9] T. Murayama, Y. Ogawa, Similar Ca^{2+} dependences of [^{3}H]ryanodine binding to alpha- and beta-ryanodine receptors purified from bullfrog skeletal muscle in an isotonic medium, FEBS Lett. 380 (1996) 267–271.
[10] I. Bezprozvanny, J. Watras, B.E. Ehrlich, Bell-shaped calcium-response curves of Ins(1,4,5)P3- and calcium-gated channels from endoplasmic reticulum of cerebellum, Nature 351 (1991) 751–754.
[11] I. Zimanyi, I.N. Pessah, Comparison of [^{3}H]ryanodine receptors and Ca^{++} release from rat cardiac and rabbit skeletal muscle sarcoplasmic reticulum, J. Pharmacol. Exp. Ther. 256 (1991) 938–946.

[12] O. Thibault, J.C. Gant, P.W. Landfield, Expansion of the calcium hypothesis of brain aging and Alzheimer's disease: minding the store, Aging Cell 6 (2007) 307–317.
[13] E.A. Sobie, L.S. Song, W.J. Lederer, Restitution of Ca(2+) release and vulnerability to arrhythmias, J. Cardiovasc. Electrophysiol. 17 (Suppl. 1) (2006) S64–S70.
[14] A.E. Rossi, R.T. Dirksen, Sarcoplasmic reticulum: the dynamic calcium governor of muscle, Muscle Nerve 33 (2006) 715–731.
[15] G. Meissner, Regulation of mammalian ryanodine receptors, Front Biosci. 7 (2002) d2072–d2080.
[16] D.R. Laver, T.M. Baynes, A.F. Dulhunty, Magnesium inhibition of ryanodine-receptor calcium channels: evidence for two independent mechanisms, J. Membr. Biol. 156 (1997) 213–229.
[17] P. Donoso, C. Hidalgo, pH-sensitive calcium release in triads from frog skeletal muscle. Rapid filtration studies, J. Biol. Chem. 268 (1993) 25432–25438.
[18] G.D. Lamb, D.G. Stephenson, Effect of Mg^{2+} on the control of Ca^{2+} release in skeletal muscle fibres of the toad, J. Physiol. 434 (1991) 507–528.
[19] P. Donoso, P. Aracena, C. Hidalgo, Sulfhydryl oxidation overrides Mg(2+) inhibition of calcium-induced calcium release in skeletal muscle triads, Biophys. J. 79 (2000) 279–286.
[20] C.F. Perez, A. Voss, I.N. Pessah, P.D. Allen, RyR1/RyR3 chimeras reveal that multiple domains of RyR1 are involved in skeletal-type E-C coupling, Biophys. J. 84 (2003) 2655–2663.
[21] D.C. Sheridan, H. Takekura, C. Franzini-Armstrong, K.G. Beam, P.D. Allen, C.F. Perez, Bidirectional signaling between calcium channels of skeletal muscle requires multiple direct and indirect interactions, Proc. Natl. Acad. Sci. USA 103 (2006) 19760–19765.
[22] Y. Wang, C. Fraefel, F. Protasi, R.A. Moore, J.D. Fessenden, I.N. Pessah, A. DiFrancesco, X. Breakefield, P.D. Allen, HSV-1 amplicon vectors are a highly efficient gene delivery system for skeletal muscle myoblasts and myotubes, Am. J. Physiol. Cell Physiol. 278 (2000) C619–C626.
[23] F. Protasi, C. Paolini, J. Nakai, K.G. Beam, C. Franzini-Armstrong, P.D. Allen, Multiple regions of RyR1 mediate functional and structural interactions with alpha(1S)-dihydropyridine receptors in skeletal muscle, Biophys. J. 83 (2002) 3230–3244.
[24] C.F. Perez, S. Mukherjee, P.D. Allen, Amino acids 1-1,680 of ryanodine receptor type 1 hold critical determinants of skeletal type for excitation-contraction coupling. Role of divergence domain D2., J. Biol. Chem. 278 (2003) 39644–39652.
[25] S.P. Brooks, K.B. Storey, Bound and determined: a computer program for making buffers of defined ion concentrations, Anal. Biochem. 201 (1992) 119–126.
[26] R.A. Moore, H. Nguyen, J. Galceran, I.N. Pessah, P.D. Allen, A transgenic myogenic cell line lacking ryanodine receptor protein for homologous expression studies: reconstitution of Ry1R protein and function, J. Cell Biol. 140 (1998) 843–851.
[27] D.R. Laver, Ca^{2+} stores regulate ryanodine receptor Ca^{2+} release channels via luminal and cytosolic Ca^{2+} sites, Clin. Exp. Pharmacol. Physiol. 34 (2007) 889–896.
[28] T. Murayama, T. Oba, E. Katayama, H. Oyamada, K. Oguchi, M. Kobayashi, K. Otsuka, Y. Ogawa, Further characterization of the type 3 ryanodine receptor (RyR3) purified from rabbit diaphragm, J. Biol. Chem. 274 (1999) 17297–17308.
[29] T. Murayama, Y. Ogawa, Characterization of type 3 ryanodine receptor (RyR3) of sarcoplasmic reticulum from rabbit skeletal muscles, J. Biol. Chem. 272 (1997) 24030–24037.
[30] S. Gyorke, D. Terentyev, Modulation of ryanodine receptor by luminal calcium and accessory proteins in health and cardiac disease, Cardiovasc. Res. (2007).
[31] A. Chugun, O. Sato, H. Takeshima, Y. Ogawa, Mg^{2+} activates the ryanodine receptor type 2 (RyR2) at intermediate Ca^{2+} concentrations, Am. J. Physiol. Cell Physiol. 292 (2007) C535–C544.
[32] G. Meissner, Ryanodine receptor/Ca^{2+} release channels and their regulation by endogenous effectors, Annu. Rev. Physiol. 56 (1994) 485–508.
[33] J.D. Fessenden, Y. Wang, R.A. Moore, S.R. Chen, P.D. Allen, I.N. Pessah, Divergent functional properties of ryanodine receptor types 1 and 3 expressed in a myogenic cell line, Biophys. J. 79 (2000) 2509–2525.
[34] R. Bull, J.J. Marengo, J.P. Finkelstein, M.I. Behrens, O. Alvarez, SH oxidation coordinates subunits of rat brain ryanodine receptor channels activated by calcium and ATP, Am. J. Physiol. Cell Physiol. 285 (2003) C119–C128.